

SPALL STRENGTH MEASUREMENTS OF EPOXY POLYMERS

Pepper, J. E.¹, Huneault, J.² Rahmat, M.³, and Petel, O. E.^{1*}

¹Department of Mechanical and Aerospace Engineering, Carleton University, Ottawa, Canada

²Department of Mechanical Engineering, McGill University, Montreal, QC, H3A 0C3, Canada

³ Aerospace, National Research Council Canada, Ottawa, Canada

* Oren E. Petel (oren.petel@carleton.ca)

Keywords: *Spall Strength · Epoxy · Plate Impact*

ABSTRACT

Dynamic tensile failure of epoxy resin cured with two different curing agents was studied in terms of spall strength. Plate impact experiments were conducted to examine how the epoxy responds to one-dimensional, high-strain rate loading. Velocity measurements of the back surface of the targets were taken during impact with a photonic-Doppler velocimeter (PDV). The velocity profiles that resulted were analyzed to gain insight on the material interface/stress wave interactions that manifested within the samples. Spall strength measurements in EPON 828 cured with EPIKURE 3223 obtained from this analysis were, on average, 29% higher than those in EPON 828 cured with EPIKURE 3233. Evidence for the existence of a quantifiable relationship between the curing agent used to cure the resin and the dynamic tensile strength of the resulting epoxy is provided. The discrepancies in the measured spall strengths between the two epoxy systems were attributed to a difference in the electrostatic forces between adjacent polymer chains within the cross-linked epoxy network. Strength measurements in both epoxies demonstrated significant strain-rate dependency. Spall strength measurements presented in this study were noticeably higher than those listed in the literature for similar thermosetting polymers.

1 INTRODUCTION

Epoxy resins are thermosetting polymers that see widespread use in industry due to their favourable mechanical properties, which include high modulus and adhesion strength, low creep at elevated temperatures, and ease of application [1]. Epoxies are comprised of two parts: a resin and a curing agent. Mixing these two parts initiates a chemical reaction that yields a polymer with a highly-crosslinked epoxy network [2]. The kinetics of this reaction have a direct effect on the mechanical properties of the resulting epoxy, whereby variables such as cure temperature, mixing rate, stoichiometric ratio, and setting time all influence the polymerization process [2,3]. Developments in composite technology, such as the introduction of nanocrystalline materials into composite systems, have led to a resurgence in research relating to the dynamic characterization of thermosetting polymers [4-8]. Relevant applications of epoxies include their use as surrogate materials for polymeric binder phases in energetic materials [9,10] and as stand-ins for transparent armour [11-13].

Carter and Marsh [14] used explosives to shock-load a selection of representative polymers. They observed high-pressure transformations in all polymers characterized by a large decrease in volume of the shocked material. They attributed these transformations to the shock-induced restructuring of the molecular backbone, where the transformation parameters were shown to be insensitive to the degree of crystallinity of the original polymer. They also ruled out the possibility of the transformation being caused by melting or vaporization, since the behaviour was observed in both thermosetting and thermoplastic polymers.

Chen et al. [15] used a modified split Hopkinson tension bar to study dynamic stress-strain responses and failure behaviour of EPON 828/T-403 epoxy. They observed that the peak tensile strengths measured for EPON 828/T-403 under dynamic loading were achieved at smaller strains when compared to the quasi-static case. Furthermore, the specimens fractured in a brittle manner during dynamic tensile loading, while the quasi-static specimens failed in a ductile manner with a necking process, thereby providing evidence for a strain-rate effect.

Millett et al. [16] investigated the effects of chemistry on the dynamic tensile failure of several polymers subjected to plate impact loading. They found that the electrostatic repulsion between adjacent polymer chains, as well as their molecular shape, influenced the shock response of the polymer. Millet and Bourne [17] also conducted plate impact experiments to study the behaviour of an epoxy resin under one-dimensional shock loading. By instrumenting the samples with longitudinal and lateral-oriented stress gauges, they successfully measured a variation of shear strength with increasing impact stress. Their results provided evidence for a shear strengthening effect that they attributed to the viscoelastic nature of epoxy resins.

Razack and Varghese [3] used thermogravimetric analysis (TGA) and differential scanning calorimetry (DSC) to investigate the effect of various hardeners (two aliphatic and two aromatic) on the properties of epoxy resin. Their results showed a clear divide in effectiveness between the thermal and mechanical performance of epoxy resin cured with aliphatic and aromatic hardeners.

Spall failure in epoxy has been studied by several researchers. Guess [18] published a spall strength of 76 MPa for EPON 828 epoxy. A later investigation by Golubev et al. [19] showed that spall strength values for most amorphous polymers typically range between 100-300 MPa, where the observed spallation characteristics change with peak pressure. Samples recovered from plate impact experiments conducted at different temperatures showed zones of increasing plasticity near crack tips. Similar experimentation conducted by Parhomenko and Utkin [20] expanded upon their findings. They published a spall strength of 300 ± 50 MPa for epoxy EDT-10.

The effect of the curing agent on the spall strengths of thermosetting polymers presents a knowledge gap in the literature, where one could expect to see an influence of the microstructure on macroscopic mechanical performance. This study seeks to fill this gap by providing insight on the effect of curing agents on the dynamic tensile properties of epoxy resin. Plate impact experiments were conducted to measure the spall strength of EPON 828 cured with two different curing agents. A discussion of the observed failure behaviour is also provided to supplement the results of this investigation.

2 MATERIALS AND METHODS

EPON 828 is an undiluted, clear, difunctional, bisphenol A liquid epoxy resin. The first curing agent was EPIKURE 3223. It is an unmodified aliphatic diethylenetriamine (DETA). The second curing agent was EPIKURE 3233, which is an unmodified aliphatic polyoxypropylenetriamine. A concise description of the physical meanings associated with the nomenclature of each compound is provided by Razack and Varghese [3]. All materials (curing agents and resin) were sourced from Hexion Inc. For clarity, the epoxies that resulted from curing EPON 828 resin with Epikure 3223 and Epikure 3233 will henceforth be referred to as EPON 828-A and EPON 828-B, respectively. A summary of the physical properties of all materials used in these experiments is provided in Table 1.

The epoxy samples used for this series of plate impact experiments were machined from cast plates. The plates were cast at room temperature and were allowed to set for enough time to ensure a 100% degree of cure. A post-cure procedure was also followed for each of the specimens based on the manufacturer's recommendation. The surfaces of the EPON 828-A samples were not polished after machining (i.e. kept in their as-machined state), whereas the front and back surfaces of the EPON 828-B targets were polished with a stepwise process that used up to 400 grit sandpaper to remove any visible surface imperfections.

Material	ρ_0 (g·cm ⁻³)	C_0 (km·s ⁻¹)	C_L (km·s ⁻¹)	Z (GPa·s·m ⁻¹)	σ_{max} (MPa)	ϵ_{max}	E (GPa)
Al 6061-T6	2.700 ^a	5.35 ^c	6.40 ^c	14.44	310 ^a	0.120 ^a	68.9 ^a
Plexiglas G	1.193 ^b	2.60 ^c	2.72 ^c	3.08	72.4 ^b	0.050 ^b	3.10 ^b
EPON 828-A	1.185 ^c	2.64 ^c	2.63 ^c	3.13	65.0	0.046	2.65
EPON 828-B	1.185 ^c	2.64 ^c	2.63 ^c	3.13	58.6	0.037	2.85

^a Glemco Inc. [21]

^b Arkema Inc. [22]

^c Marsh [23]

Table 1. The relevant physical properties of all materials used in the plate impact experiments, where ρ_0 is bulk density, C_0 is bulk sound speed, C_L is longitudinal sound speed, Z is specific acoustic impedance, σ_{max} is maximum tensile strength, ϵ_{max} is strain achieved at the maximum tensile strength, and E is tensile modulus.

A single-stage light gas gun with an internal bore of 64 mm was used for this series of impact experiments. The gun generated projectile impact velocities between 136 and 715 ms⁻¹. A schematic of the target assembly mounted on the gas gun is shown in Figure 1. The cylindrical projectiles comprised of a plastic (nylon or PVC) sabot fitted with a flyer plate made from either PMMA or aluminum 6061-T6. The aluminum and PMMA flyer plates were laser cut from 1.96 mm and 1.55 mm sheet stock, respectively. A relief port was drilled through the wall of the sabot into an air gap located directly behind the flyer plate. The purpose of this relief port was to allow the gas pressure on both sides of the flyer plate to equilibrate during the evacuation of the catch tank, which helped to eliminate any undesired flexing/loading of the flyer plate. A schematic of the projectile is shown in Figure 1. Prior to launching the projectile, the catch tank was evacuated to an operating pressure of approximately 150 Pa.

The impact of the test samples was observed with a two-channel photonic-Doppler velocimeter (PDV) [24,25] and a piezoelectric (shock) pin arranged in the configuration shown in Figure 1. The shock pin was mounted flush with the front face of the target. It was used to gauge the exact instant of impact and to trigger the acquisition of the PDV data. The PDV was used to measure the velocity of the back surface of the target and the velocity of the flyer plate. This was achieved using separate collimators. The velocity history of the flyer plate was monitored by a spotting laser projected through a hole drilled into the target. The spotting laser was also used to provide an ancillary method of identifying the time of arrival (TOA) of the flyer plate.

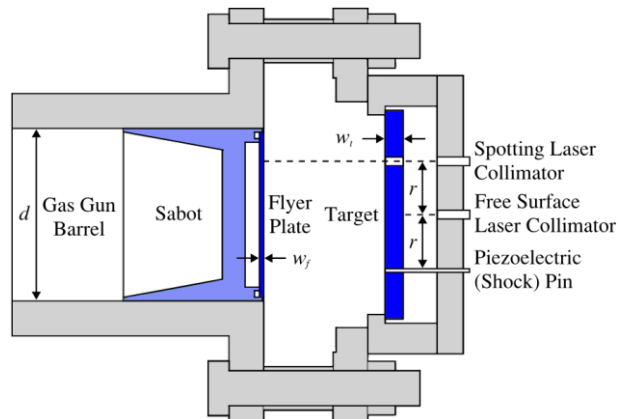


Figure 1. A schematic of the target assembly mounted at the end of the gas gun barrel, where $d = 64$ mm, $r = 25.4$ mm, and $w_f = 1.96$ or 1.55 mm.

The PDV used in this study has a 550 nm infrared laser; however, EPON 828 is not infrared-reflective, which made it impossible to take direct measurements of the free surface velocity during impact. It was therefore necessary to introduce a reflective buffer material to the back face of each sample. This was achieved by using a semicore inline sputtering system to coat the back surface of each sample with a 40-60 nm layer of aluminum 6061-T6. This process required the samples to be held in a vacuum chamber for several hours to allow for sufficient degassing of the material, followed by the coating process, which occurred at an operating temperature of 50°C. It was found that the quality (i.e. reflectivity) of the aluminum coating improved if the samples were polished prior to subjecting them to the sputtering system.

3 THEORY

The primary wave interactions within the target for a spall test are illustrated in Figure 2, where the relationship between the specific acoustic impedances (Z) of the flyer plate and target influence the nature of these wave interactions [26]. The interactions of the rarefaction fans may result in the generation of a large tensile stress within the sample. If this tensile stress exceeds the local strength of the material, and partial or complete fracture is observed, then either incipient or total spall failure is said to have occurred [27-31]. The magnitude of the tensile stress that produces any degree of spall failure is designated as the spall strength of the target material [27-31]. Therefore, spall failure can be defined as dynamic tensile failure caused by the interaction of rarefaction waves within a material that are generated during high-strain rate deformation [28]. Spall strength is often used in combination with parameters such as fracture toughness, ballistic limit, energy absorption, hardness, etc. to quantify resistance to dynamic failure caused by ballistic impact.

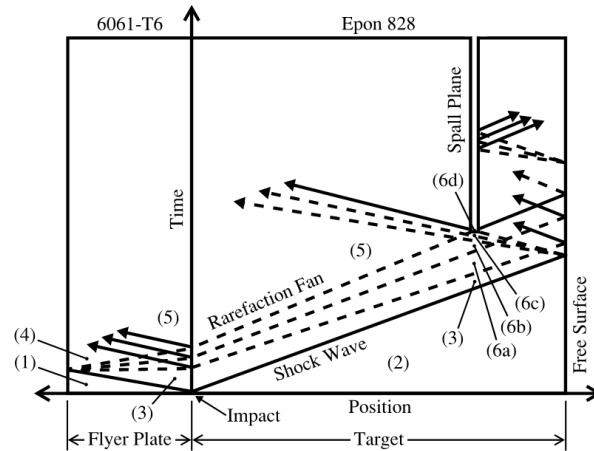


Figure 2. A position-time plot depicting the wave interactions that occur during an asymmetrical plate impact, meaning that the flyer plate has a higher specific acoustic impedance than the target. Dash lines represent rarefaction wavelets, while solid lines represent shock/compression waves.

Given that spall failure is the result of wave interactions involving significant material motion, the spall strength of a material is determined from the velocity profile of the back (free) surface of the sample. The features of the velocity profile are directly representative of the interactions between the compressive shock waves, rarefaction fans, and target interfaces during impact [28,31]. A schematic free surface velocity profile is shown in Figure 3. The post-shock peak velocity (u_{peak}) is given by [26]

$$u_{peak} \approx 2u_p, \quad (1)$$

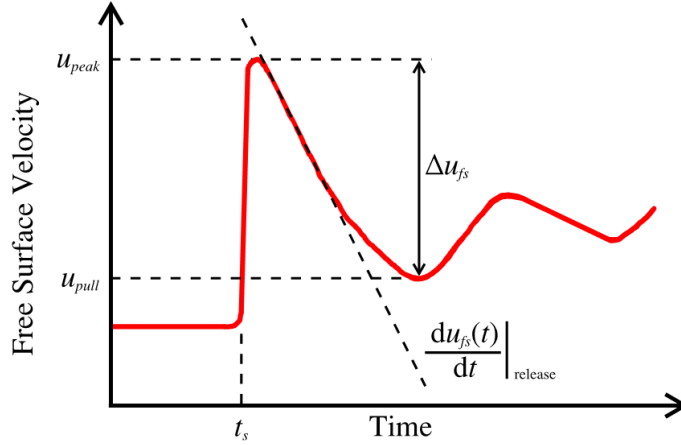


Figure 3. A schematic plot of a free surface velocity profile obtained from a spall experiment.

where u_p is the particle velocity off the free surface of the target. The spall strength (σ_{sp}) of the target material can be predicted from the free surface velocity profile using an acoustics approach that gives the well-known linear approximation [31,32]

$$\sigma_{sp} = \rho_0 C_L \Delta u_{fs} \frac{1}{1 + \frac{C_L}{C_0}}, \quad (2)$$

where ρ_0 is bulk density, C_L is longitudinal sound speed, C_0 is bulk sound speed, and Δu_{fs} is the characteristic change in the free surface velocity observed on the velocity profile. The Δu_{fs} term is determined by [32]

$$\Delta u_{fs} = u_{peak} - u_{pull}, \quad (3)$$

where the peak velocity (u_{peak}) and the pullback velocity (u_{pull}) are read directly off the free surface velocity profile (see Figure 3). The strain rate achieved during the release (i.e. decompression) stage is given by [33]

$$\dot{\epsilon}_r \approx \frac{1}{2C_0} \left. \frac{du_{fs}(t)}{dt} \right|_{release}. \quad (4)$$

The spall strengths of many materials exhibit strain-rate dependency [31]. Spall strength can be used to quantify dynamic tensile failure in the epoxy, and hence evaluate its ability to resist ballistic impacts that fall within a predefined regime of strain rates and stress states.

4 RESULTS AND DISCUSSION

Processing the PDV data begins by reading out a binary waveform from the oscilloscope that was used to collect the raw PDV diagnostic data. An example of a binary waveform retrieved from the raw PDV data is shown in Figure 4(a). The binary waveform is then treated with a windowed Fourier transform that returns a spectrogram showing a distribution of laser beat frequencies, where the peak frequency is associated with the motion of the target material. The spectrogram that corresponds to the waveform in Figure 4(a) is shown in Figure 4(b). This process was followed for each shot. Four representative spectrograms retrieved from the series of plate impact experiments are presented in Figures 5 and 6. A discussion of their features is provided below.

The reader is first asked to observe the large horizontal signal bands present in the EPON 828-A spectrograms in Figures 5(a) and 5(b). It is believed that these bands can be attributed to the formation of aluminum ejecta plumes at the back face of the targets, where the PDV registered a spectrum of velocities spanned by a cloud of aluminum particles ejected from the back face, post-shock arrival. Similar PDV signals have previously been reported for ejecta plumes [34]. This ejecta formation could be due to one of a few mechanisms, but it is most likely that excessive shear generated at the aluminum/epoxy interface was caused by interactions between the shock waves/rarefaction fans and the rough surface [34]. As mentioned earlier, the surfaces of the EPON 828-B targets were polished prior to coating with the sputtering system, whereas the surfaces of the EPON 828-A targets were not. It was evident that the rougher surfaces on the EPON 828-A targets resulted in an aluminum finish of lesser

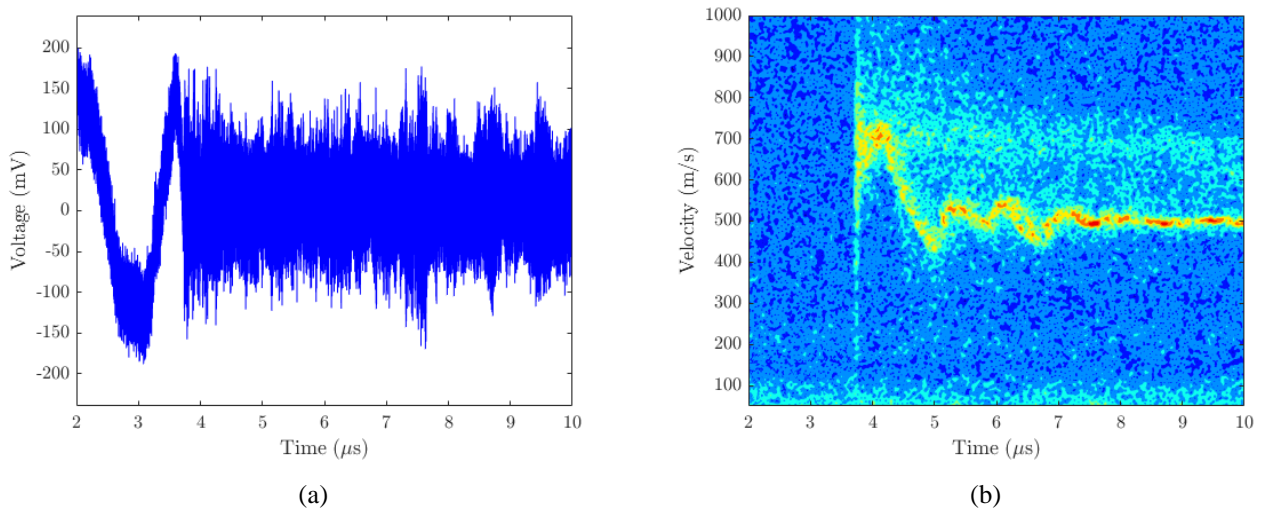


Figure 4. (a) The binary waveform retrieved from the raw PDV signal of an EPON 828-B target impacted with a PMMA flyer plate at a velocity of 638 ms^{-1} . (b) The spectrogram associated with the binary waveform in Figure 4(a).

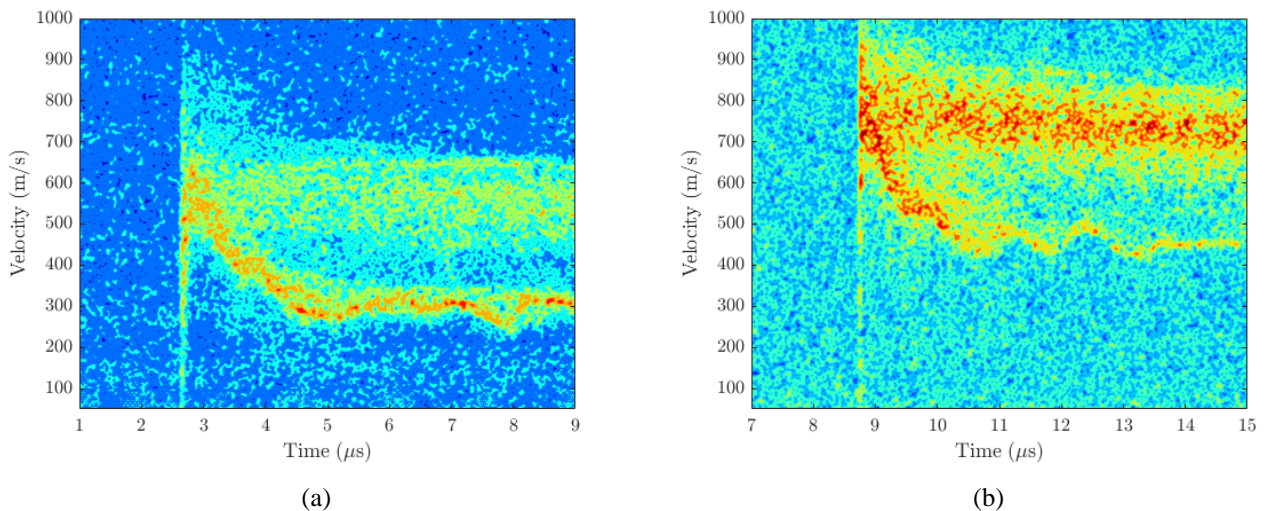


Figure 5. (a) An EPON 828-A target impacted with an aluminum 6061-T6 flyer plate at a velocity of 363 ms^{-1} . (b) An EPON 828-A target impacted with an aluminum 6061-T6 flyer plate at a velocity of 503 ms^{-1} .

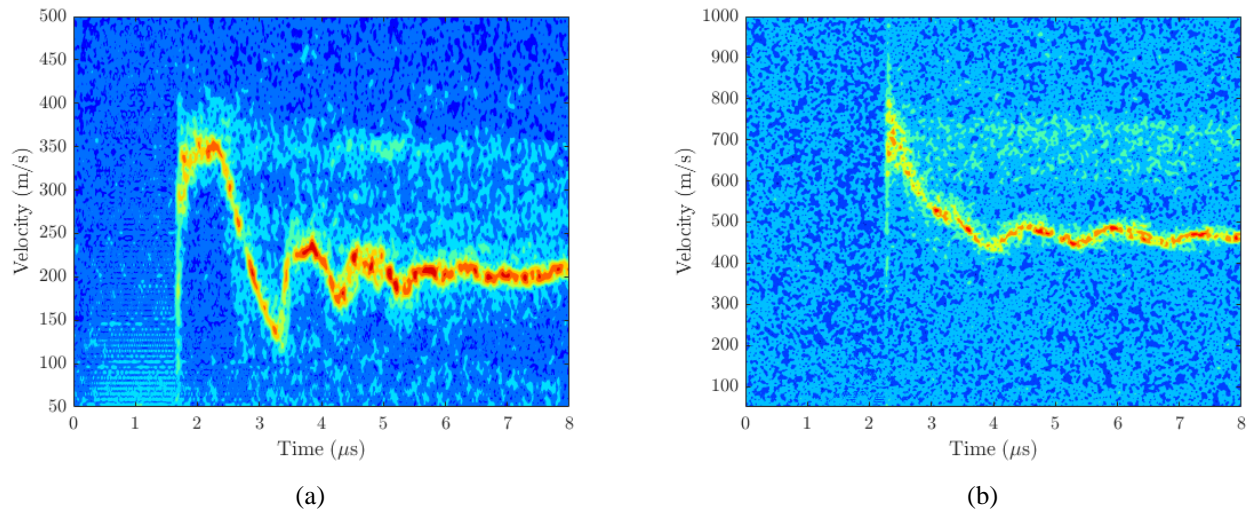


Figure 6. (a) An EPON 828-B target impacted with a PMMA flyer plate at a velocity of 344 ms^{-1} . (b) An EPON 828-B target impacted with an aluminum 6061-T6 flyer plate at a velocity of 471 ms^{-1} .

quality. Upon observation of the spectrograms presented in Figures 5 and 6, it is apparent that the resolution of the velocity profiles for the EPON 828-B targets is better than the resolution of their EPON 828-A counterparts. It is also evident that larger ejecta plumes were formed from the EPON 828-A targets, which had rougher back surfaces. This suggests a link between the pre-coating surface roughness and the shear generated at the aluminum/epoxy interface, and by proxy, an effect of the surface roughness on the resolution of the velocity signal.

Difficulty arose when attempting to identify the correct peak velocity (u_{peak}) seen on the free surface velocity profiles due to the aforementioned-scatter in the velocity signal. Therefore, it was necessary to validate the peak velocities. This was achieved by following the analytical procedure described by Cooper [26], which first estimates the particle velocity (u_p) of the material behind the initial shock front traveling through the target, and then utilizes Eq. (1) to determine the expected peak velocity. Using this procedure, the estimated and observed peak velocities were found to be in good agreement.

The reader is now asked to notice the stepwise deceleration of the free surface velocity seen in Figures 5(a), 5(b), and 6(b). The presence of these plateaus complicated the process of identifying the correct pullback velocity (u_{pull}). It was believed that the plateaus were caused by the impedance mismatch between the aluminum flyer plates and the epoxy targets [26]. This was confirmed by analyzing the velocity profiles obtained from shots conducted under identical conditions but using different flyer plate materials. Shots conducted with PMMA flyer plates did not yield velocity profiles with a stepwise deceleration during the release stage, whereas shots conducted with aluminum 6061-T6 flyer plates did. This can be verified by examining Figures 4(b) and 6(a), which do not possess a plateau during the release stage. Therefore, it can be concluded that the plateaus are indeed caused by the impedance mismatch between the flyer plate and target materials, and hence that it was correct to take u_{pull} as the velocity achieved at the deepest valley on the velocity profile during the release stage.

An analysis of the velocity profiles retrieved from experimentation was conducted to determine the dynamic tensile strengths of EPON 828-A and EPON 828-B, which can be used to quantify their failure behaviour when subjected to one-dimensional, high-strain rate loading. The results of these analyses are presented graphically in Figure 7 and quantitatively in Table 2.

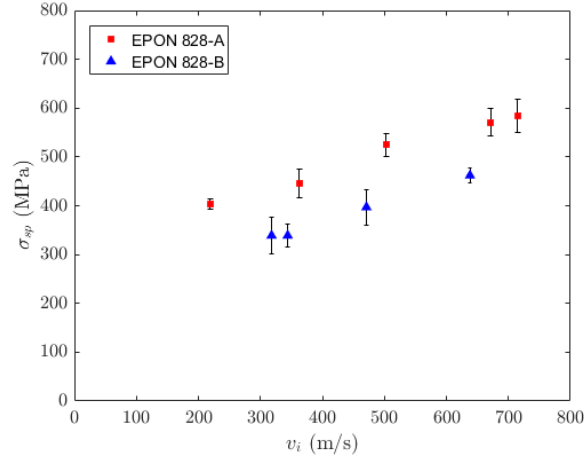


Figure 7. Spall strength measurements plotted against impact velocity for EPON 828-A and EPON 828-B.

Both EPON 828-A and EPON 828-B demonstrated significant strain rate sensitivity, where all spall strength measurements were approximately one order of magnitude greater than the quasi-static max tensile strengths listed for both materials (see Table 1). A positive correlation between spall strength and impact velocity is also observed. Most importantly, Figure 7 shows that EPON 828-A has a consistently higher spall strength than EPON 828-B for experiments conducted at similar impact velocities. Therefore, it is reasonable to conclude that the choice of curing agent has a direct effect on the dynamic tensile performance of the resultant epoxy. The results of this study contrast directly with those of Guess [18] who published a spall strength of 76 MPa for EPON 828 epoxy. A likely explanation for this discrepancy between the results of the present study and those of reported by Guess in 1968 is likely the strong influence of the curing agent on the spall strength, as seen in Figure 7, where the spall strength of EPON 828-A was, on average, 29% higher than that of EPON 828-B. Such a large difference between contemporary curing agents for a resin system, which have been optimized throughout years of research may explain the even larger variation between the results of Guess and the present study.

Target Material	w_t (mm)	Flyer Material	v_i (m·s ⁻¹)	Δu_{fs} (m·s ⁻¹)	σ_{sp} (MPa)	$\dot{\epsilon}_r$ (s ⁻¹)
EPON 828-A	5.44	PMMA	136	N.S.	-	-
EPON 828-A	6.50	Al 6061-T6	219	259	404	3.22×10^4
EPON 828-A	5.38	Al 6061-T6	363	285	445	4.00×10^4
EPON 828-A	6.58	Al 6061-T6	503	336	525	4.53×10^4
EPON 828-A	6.43	Al 6061-T6	671	366	571	5.53×10^4
EPON 828-A	6.27	Al 6061-T6	715	375	585	7.64×10^4
EPON 828-B	6.68	PMMA	344	217	339	5.16×10^4
EPON 828-B	6.53	PMMA	638	296	462	7.00×10^4
EPON 828-B	6.58	Al 6061-T6	118	N.S.	-	-
EPON 828-B	6.58	Al 6061-T6	318	217	339	3.08×10^4
EPON 828-B	6.60	Al 6061-T6	471	254	397	5.57×10^4

Table 2. The quantitative results of the plate impact experiments, where w_t is target thickness and v_i is impact velocity. The term N.S. refers to a no-spall shot, where the characteristic pullback signal was not observed on the velocity profile.

A different explanation might be the effect of the choice of flyer plate material on the interpretation of the spall signal. The flyer plate material will influence the back face the velocity profile, which can lead to the misidentification of the pullback velocity. Meanwhile, the spall strength of 300 ± 50 MPa published in 1990 by Parhomenko and Utkin [20] for epoxy EDT-10 is within the same order of magnitude as the strengths reported in the present study for EPON 828. Their results simply exemplify the large potential for variation in strength that can be observed between epoxy systems.

Such a result makes it necessary to examine the distinguishing features of these two curing agents with the intention of isolating the variable with the single highest potential to influence microstructure. Millett et al. [16] demonstrated that variation in the atoms attached to the polymer backbone in thermoplastics can change their macroscopic dynamic behaviour. Similar experimentation could be used to see if the same is true for thermosetting polymers. A series of impact experiments could also be used to identify the parameter with the single greatest influence on the microstructure. Successful identification of this parameter would suggest the potential to control the dynamic tensile performance of the cured epoxy. Support for this claim could be provided by comparing the results obtained from differential scanning calorimetry and/or thermogravimetric analysis of the epoxy samples.

5 CONCLUSIONS

The objective of this series of plate impact experiments was to investigate the dynamic tensile behaviour of EPON 828 resin cured with two different curing agents. This was achieved by subjecting EPON 828 resin cured with EPIKURE 3223 and EPIKURE 3233 to one-dimensional, high-strain rate loading and then analyzing the associated free surface velocity profiles that were obtained using the PDV. The properties of both epoxy systems demonstrated high degrees of strain rate sensitivity. It was also apparent that the choice of curing agent had a significant effect on dynamic tensile failure of the resulting epoxy, where the spall strengths measured for both epoxy systems demonstrated consistent variation across a range of impact velocities. Further investigation would be required to confidently identify the root cause of the observed results.

6 ACKNOWLEDGMENTS

The authors would like to thank Andrew Higgins for granting access to his research facility. Financial support by the National Research Council Canada through the Security Materials Technology program is also appreciated.

7 REFERENCES

- [1] J. Kinloch, R. D. Mohammed, A. C. Taylor, C. Eger, S. Sprenger and D. Egan. "The effect of silica nano particles and rubber particles on the toughness of multiphase thermosetting epoxy polymers." *Journal of Materials Science*, Vol. 40, No. 18. pp 5083-5086, 2005.
- [2] L. Wu, S. V. Hoa and M. T. Ton-That. "Effects of composition of hardener on the curing and aging for an epoxy resin system". *Journal of Applied Polymer Science*, Vol. 99, No. 2, pp 580-588, 2006.
- [3] N. A. Razack and L. A. Varghese. "The effect of various hardeners on the mechanical and thermal properties of epoxy resin". *International Journal of Engineering Research and Technology*, Vol. 3, No. 1, pp 2662-2665, 2014.
- [4] M. G. Stout, D. A. Koss, C. Liu and J. Idasetima. "Damage development in carbon/epoxy laminates under quasi-static and dynamic loading". *Composite Science and Technology*, Vol. 59, No. 16, pp 2339-2350, 1999.
- [5] D. P. Dandekar, C. A. Hall, L. C. Chhabildas and W. D. Reinhart. "Shock response of a glass-fiber-reinforced polymer composite". *Composite Structures*, Vol. 61, No. 1-2, pp 51-9, 2003.
- [6] E. Zaretsky, G. DeBotton and M. Perl. "The response of a glass fibers reinforced epoxy composite to an impact loading". *International Journal of Solids and Structures*, Vol. 41, No. 2, pp 569-584, 2004.
- [7] R. E. Setchell and M. U. Anderson. "Shock-compression response of an alumina-filled epoxy". *Journal of Applied Physics*, Vol. 97, No. 8 (083518), 2005.

- [8] F. Yuan, L. Tsai, V. Prakash, A. M. Rajendran and D. P. Dandekar. "Spall strength of glass fiber reinforced polymer composites". *International Journal of Solids and Structures*, Vol. 44, No. 24, pp 7731-7747, 2007.
- [9] D. M. Hoffman. "Dynamic mechanical signatures of viton A and plastic bonded explosives based on this polymer". *Polymer Engineering & Science*, Vol. 43, No. 1, pp 139-156, 2003.
- [10] A. Milne, A. Longbottom, N. K. Bourne and J. C. F. Millett. "On the unreacted Hugoniot of three plastic bonded explosives". *Propellants, Explosives, Pyrotechnics*, Vol. 32, No. 1, pp 68-72, 2007.
- [11] M. Grujicic, W. C. Bell and B. Pandurangan. "Design and material selection guidelines and strategies for transparent armor systems". *Materials & Design*, Vol. 34, pp 808-819, 2012.
- [12] P. J. Hazell. "Armour: materials, theory, and design". 1st edition, CRC Press, 2015.
- [13] P. J. Patel, A. J. Hsieh and G. A. Gilde. "Improved low-cost multi-hit transparent armor". U. S. Army Research Laboratory, Aberdeen Proving Ground, MD, 2006.
- [14] W. Carter and S. P. Marsh. "Hugoniot equation of state of polymers". Los Alamos National Laboratory, Los Alamos, NM, 1995.
- [15] W. Chen, F. Lu and M. Cheng. "Tension and compression tests of two polymers under quasi-static and dynamic loading". *Polymer Testing*, Vol. 21, No. 2, pp 113-121, 2002.
- [16] J. C. F. Millett, E. N. Brown, G. T. Gray, N. K. Bourne, D. C. Wood and G. Appleby-Thomas. "The effects of changing chemistry on the shock response of basic polymers". *Journal of Dynamic Behavior of Materials*, Vol. 2, No. 3, pp 326-336, 2016.
- [17] J. C. F. Millett, N. K. Bourne and N. R. Barnes. "The behavior of an epoxy resin under one-dimensional shock loading". *Journal of Applied Physics*, Vol. 92, No. 11, pp 6590-6594, 2002.
- [18] T. R. Guess. "Some dynamic mechanical properties of an epoxy". SC-DR-68-343, Sandia Laboratories, Albuquerque, NM, 1968.
- [19] V. K. Golubev, S. A. Novikov and Y. S. Sobolev. "Effect of temperature on spall of polymer materials". *Journal of Applied Mechanics and Technical Physics*, Vol. 23, No. 1, pp 134-141, 1982.
- [20] I. P. Parhomenko and A. V. Utkin. "Matter under extreme conditions". IVTAN, Moscow, RU, pp 126-130, 1990.
- [21] Specification Sheet. "6061-T6 Aluminum". Glemco Inc., Leander, TX.
- [22] Specification Sheet. "Plexiglas G". Arkema Inc., Bristol, PA, 2013.
- [23] S. P. Marsh. "LASL Shock Hugoniot Data". University of California Press, Berkeley, 1980.
- [24] L. M. Barker and R. E. Hollenbach. "Laser interferometer for measuring high velocities of any reflecting surface". *Journal of Applied Physics*, Vol. 43, No. 11, pp 4669-4675, 1972.
- [25] O. T. Strand, L. V. Berzins, D. R. Goosman, W. W. Kuhlow, P. D. Sargis and T. L. Whitworth. "Velocimetry using heterodyne techniques". Lawrence Livermore National Laboratory, Livermore, CA, 2004.
- [26] P. W. Cooper. "Explosives Engineering". 4th edition, Wiley-VCH, 2002.
- [27] G. I. Kanel, S. V. Razorenov and V. E. Fortov. "Shock-wave phenomena and the properties of condensed matter". 1st edition. Springer Science & Business Media, 2004.
- [28] M. A. Meyers and C. T. Aimone. "Dynamic fracture (spalling) of metals". *Progress in Materials Science*, Vol. 28, No. 1, pp 1-96, 1983.
- [29] P. Chevrier and J. R. Klepaczko. "Spall fracture: mechanical and microstructural aspects". *Engineering Fracture Mechanics*, Vol. 63, No. 3, pp 273-294, 1999.
- [30] G. I. Kanel. "Spall fracture: methodological aspects, mechanisms and governing factors". *International Journal of Fracture*, Vol. 163, No. 1, pp 173-191, 2010.
- [31] T. Antoun, L. Seaman, D. R. Curran, G. I. Kanel, S. V. Razorenov and A. V. Utkin. "Spall fracture". 1st edition, Springer-Verlag, 2006.
- [32] G. V. Stepanov. "Spall fracture of metals by elastic-plastic loading waves". *Problemy Prochnosti*, Vol. 8, pp 66-70, 1976.
- [33] S. N. Luo, Q. An, T. C. Germann and L. B. Han. "Shock-induced spall in solid and liquid Cu at extreme strain rates". *Journal of Applied Physics*, Vol. 106, No. 1 (013502), 2009.
- [34] G. Prudhomme, P. Mercier and L. Berthe. "PDV experiments on shock-loaded particles". *Proceedings of the Journal of Physics Conference Series*, Seattle, Vol. 500, 142027, pp 1-6, 2014.